of detection of the extent of the region affected by injury.[14] In addition, FA values were associated with motor scores showing that FA can provide information on lesion evolution and functional outcome.[14] Similarly, DTI has been shown to increase sensitivity of detection of spinal cord pathology in persons with various myelopathies compared with conventional imaging.[13,15–17] In persons with chronic SCI, decreased FA values in areas remote from the visible lesion on T2W images have been interpreted as identifying regions in which wallerian degeneration was occurring secondary to the injury.[17,18]

While both FA and ADC/MD values can typically differentiate SCI and control populations, FA has been shown to correlate with motor and sensory function, suggesting it is the more useful quantitative imaging parameter.[16–19] Tractography has been used to visualize the continuity or disruption of fibers across an area of injury in experimental SCI and in persons with SCI, but the relationship between lesion continuity and functional status has not been evaluated extensively.[16,20]

DTI has been reported in normal dogs with values established for quantitative parameters for the cervical and thoracolumbar spinal cord.[21–23] There are limited reports of DTI in dogs with SCI and these primarily include dogs with acute SCI.[22,24,25] There are no studies specifically examining DTI in chronically paralyzed dogs secondary to prior acute SCI. Further exploration of the utility of DTI in this population is warranted with the goals of improving delineation of injury and characterization of injury severity.

We hypothesized that SCI severity quantified by DTI would be associated with hindlimb motor function. Our aims in this study were to perform DTI in a population of chronically impaired dogs, to generate FA and MD values cranial, caudal, and within the lesion, to use tractography to determine integrity through the lesion epicenter, and to investigate associations between DTI indices and motor function. Establishing the relationship between DTI characteristics and motor function will enhance the utility of using dogs as a model of chronic paralysis by providing a means by which to stratify cases based on lesion severity and to track the effects of interventional clinical trials.

Methods

Control dogs

Clinically normal, adult dogs were recruited prospectively to establish normal values for quantitative DTI analysis performed using the same protocol on the same magnet as dogs with SCI. Informed consent was obtained, and examinations were conducted in accordance with the North Carolina State University Institutional Animal Care and Use Committee (protocol #15-150-O). All dogs had to have a normal neurological examination and no history of neurological disease.

Case selection

Dogs were recruited prospectively from the patient pool of the Canine Spinal Cord Injury Program at the North Carolina State University (NCSU) College of Veterinary Medicine and via trial advertisement online (https://cvm.ncsu.edu/research/labs/clinical-sciences/canine-spinal-cord-injury/, www.dodgerslist.com). Previous open field gait score (OFS) data from a comparable population (based on inclusion criteria) were used to determine that 20 dogs would allow detection of a three-point difference in mean OFS between dogs with and without intact translesional fibers with a power of 90%. Given the lack of preliminary DTI data, we aimed to enroll a minimum of 20 dogs.

To be included, dogs must have been between one and 12 years of age, suffered an acute, clinically complete (hindlimb paralysis with loss of pain perception) thoracolumbar SCI, and demonstrated an incomplete recovery at least three months after injury characterized by chronic motor deficits and severely reduced to absent hindlimb and tail pain perception (with or without urinary and fecal incontinence). Prior advanced imaging (computed tomography or MRI) at the time of injury, or definitive diagnosis were not required for inclusion. Exclusion criteria included implants that could generate MRI artifact, comorbidities precluding general anesthesia, and aggression or anxiety preventing gait analysis and handling.

Data collection on each dog included signalment, diagnosis, lesion location, duration of injury (interval from acute injury to imaging), and prior treatment of the SCI. Previous therapy including participation in interventional clinical trials were noted but not utilized as exclusion criteria for the purposes of this study. Informed consent was obtained for all animals, and examinations were conducted in accordance with the NCSU Institutional Animal Care and Use Committee (protocol #15-004-01).

General neurologic and gait evaluation. All dogs underwent a neurological examination including standard evaluation of gait, proprioception, spinal reflexes, and pain perception. More extensive gait analysis consisted of walking each dog on a nonslip surface for approximately 3 min. All examinations were videotaped. Gait was categorized as ambulatory (able to take at least 10 consecutive weight bearing steps unassisted), or not and quantified using an ordinal gait scale (open field score, OFS, ranging from 0–21).[26,27] OFS greater than 4 corresponds to taking weight bearing steps more than 10% of the time.

Imaging acquisition and processing. All dogs (cases and controls) were anesthetized and scanned in dorsal recumbency. Premedication consisted of intravenous (IV) dexmedetomidine (Dexdomitor, Orion Pharma, Espoo, Finland) 1–2 μg/kg and IV butorphanol (Torbugesic, Zoetis, Kalamazoo, MI) 0.1–0.2 mg/kg followed by propofol induction (PropoFlo 10 mg/mL, Abbott Laboratories, North Chicago, IL) and inhaled isoflurane for maintenance (VET ONE Fluriso, MWI, Boise, ID).

All MRIs were performed using a 1.5T scanner (Symphony; Siemens Medical Solutions USA Inc., Malvern, PA) using circularly polarized spine array and body array flex coils with acquisition of standard transverse and sagittal sequences (T1W pre- and post-contrast, T2W, STIR, half-Fourier acquisition single-shot turbo spin-echo (HASTE)) of the thoracolumbar spinal cord.[28] Additional sequences utilized in some, but not all, dogs included proton density and GRE/T2*.

DTI was obtained for the same region in the transverse plane using a protocol adapted from Jones and associates[29] with 35 diffusion directions with a scan time of approximately 5 min (Table 1). Five B0 nondiffusion weighted images were acquired with diffusion weighted

Table 1. Diffusion Tensor Imaging Protocol Parameters

Imaging plane	Transverse
Slice thickness (mm)	3.5
Voxel dimensions	2.5 × 2.5 × 3.5
Number of diffusion directions	35
Number of slices	50
Field of view	240 × 240
Averages	1
TR (msec)	7700
TE (msec)	100
b value (s/mm ^{2})	1000
Scan time (min)	5

TR, repetition time; TE, echo time.

FIG. 1. Example of an unprocessed, transverse diffusion-weighted image. A, anterior; L, left; R, right.

scans, and an unprocessed, transverse diffusion-weighted image is presented in Figure 1. Signal to noise ratio (SNR) was calculated on the raw diffusion weighted images ($b = 1000$ s/mm^2) by creating a region of interest (ROI) in the region with highest intensity and one in the background. SNR was defined as the ratio of the mean of the highest intensity values to the standard deviation (SD) of the background values. Post-processing of the diffusion data consisted of conversion from DICOMs to 4D image volumes using MRI Convert and storage in NIfTI format. A diffusion tensor model was fitted to these images using Diffusion Toolkit (http://trackvis.org/dtk/), providing a matrix-valued tensor for each voxel that was used to compute standard indices.

Imaging analysis

Standard MRIs were used to identify relevant anatomy and identify the lesion in cases. Post-processed DTI images were imported into Mango (http://ric.uthscsa.edu/mango/) to outline ROI on which quantitative analyses were then performed. In cases, ROI were hand drawn using B0 nondiffusion weighted transverse images at the lesion epicenter as well as one to two vertebral segments cranial and caudal to the visible extent of the lesion in normal-appearing areas on conventional MRI (T2W images). Each ROI was composed of the two-dimensional cross-sectional area of spinal cord on three consecutive slices to create a volume of tissue for analysis. Care was taken when drawing ROI to exclude extramedullary structures including cerebrospinal fluid and epidural fat.

Quantitative analysis consisted of calculation of FA and MD for each ROI constructed (cranial, lesion epicenter, caudal). Average FA and MD were calculated on corresponding ROI in controls to generate normal canine values along the thoracolumbar spinal cord using this protocol and to allow comparison to cases. Qualitative analysis consisted of generating maps of the orientation of tensors across all voxels. These tensor maps were used to perform tractography using TrackVis (http://trackvis.org) in which fiber tracts representing axonal connections were generated by tracing adjacent tensors with similar directions. Tractography provided a visual representation of the spinal cord and was assessed visually for continuity of white matter tracts across the lesion. Tractography was also performed in controls.

Statistical analysis

Analyses were performed using Jmp 12 Pro (SAS Institute, Cary, NC). Summary statistics for continuous data (FA and MD values, OFS) were reported as mean and SD if distributed normally or median and range if not using the Wilk-Shapiro test for normality. Translesional fibers were noted to be present or absent based on tractography. The FA and MD values were compared between cases and controls using the Wilcoxon rank sum test. Among cases, a model was constructed that incorporated age (categorical, ≤5 or >5 years old) and duration of injury (continuous, in months) as covariates with OFS. Using this model, relationships between FA or MD and OFS were investigated by performing an analysis of covariance. The association between the presence of translesional fibers and OFS was evaluated by Wilcoxon rank sum. A $p < 0.05$ was considered significant with adjusted p values calculated to account for multiple comparisons using the Holm correction calculator.

Results

Clinical information for controls

Six neurologically normal adult dogs were enrolled (Supplementary data 1). Median body weight was 12.5 kg (6.3–41). Mean age was 6.5 years (SD 2.7).

Clinical information and gait scoring in cases

Twenty-two dogs with SCI were enrolled. There were nine dachshunds, six mixed breed dogs, three pit bull terriers, two Australian cattle dogs, and one each of Shih Tzu and Boston terrier. Median body weight was 9.25 kg (range 4.6–38). The mean age was 5.5 years (SD 2.3), and median duration of injury was 15.5 months (range 3–84). Intervertebral disc herniation (IVDH) was the most common diagnosis (17 dogs) followed by vertebral column fracture (three dogs), fibrocartilaginous embolism (one dog), and traumatic disc extrusion (one dog). In all dogs, neurolocalization was between the third thoracic and third lumbar spinal cord segments based on neurological examination findings.

Twenty-one dogs had no pelvic limb or tail pain perception while one dog had a severely blunted response in the toes of the left hindlimb. The median OFS for all dogs was 2 (range 0–6). Two dogs were independently ambulatory (OFS 5 and 6), three dogs took some weight bearing steps (OFS 4), and 17 were nonambulatory (OFS 0-3). Treatments at the time of acute injury were variable and depended on the underlying cause. Among dogs with a diagnosis of IVDH or fracture/luxation, surgery (decompression ± stabilization) was performed in 10 dogs, and medical management with or without formal rehabilitation therapy was performed in 10 dogs.

Imaging results in controls

Conventional MRI sequences revealed no apparent lesions of the thoracolumbar spinal cord. Diffusion imaging captured a region ranging from T8–10 vertebrae cranially through L3–6 caudally, with variation in length imaged depending on the size of the dog. Mean SNR in control dogs was 28 (SD 7.3) with a minimum value of 18. Quantitative calculations and tractography were performed in all control dogs. The cranial ROI ranged from T11–12, middle ROI from T13–L2, and caudal ROI from L2–4, with each individual ROI drawn within the spinal cord at the level of the midvertebral body. Median ROI size across all spinal cord locations was 26 pixels and ranged from 18 to 46. The FA and MD values for controls are outlined in Table 2. The FA and MD values were not different between cranial, middle, and caudal ROI in controls ($p = 0.85$, $p = 0.36$,

Table 2. Summary of Median (range) Fractional Anisotropy and Mean Diffusivity Values in Controls and Cases

	Cranial ROI	Middle/lesion ROI	Caudal ROI	Overall (controls only)
FA				
Controls	0.601 (0.578–0.774)	0.611 (0.554–0.826)	0.589 (0.342–0.817)	0.602 (0.342–0.826)
Cases	0.420 (0.391–0.561)	0.228 (0.107–0.432)	0.369 (0.265–0.513)	
MD				
Controls	1.31 × 10^{-3} (.986–1.41)	1.29 × 10^{-3} (0.826–1.35)	1.13 × 10^{-3} (0.816–1.44)	1.28 × 10^{-3} (0.816–1.44)
Cases	1.52 × 10^{-3} (1.02–1.87)	2.06 × 10^{-3} (1.33–2.96)	1.31 × 10^{-3} (0.828–1.08)	

ROI, region of interest; FA, fractional anisotropy; MD, mean diffusivity.

respectively). Therefore, combined overall FA and MD for controls were used for comparison with cases. Tractography revealed uniform fiber distribution in control dogs (Fig. 2 A,B).

Imaging results in cases

Conventional MRIs identified the lesion in all cases. Lesion location ranged from the level of thoracic vertebra T7 to lumbar vertebra L4, with 13 dogs having lesions at T12–13 or cranial and nine dogs with lesions at T13–L1 or caudal. The DTI was centered over the lesion epicenter for each dog and extended from T3–7 across all cases. Diffusion imaging was of adequate quality to perform quantitative analysis and tractography in all cases. Mean SNR for cases was 29 (SD 5.2) with a minimum value of 20.5.

One dog had a lesion that extended to the cranial aspect of the window imaged and prevented drawing a ROI cranial to the visible

FIG. 2. Tractography in controls and cases. Sagittal (A) and dorsal (B) views in normal dogs showing normal fiber density and distribution. (C–F) Tractography in dogs with spinal cord injury showing varying degrees of fiber thinning and disruption. Sagittal (C) and dorsal (D) views showing moderate fiber thinning. Sagittal (E) and dorsal (F) views showing absence of translesional fibers in a dog secondary to intervertebral disc herniation. Blue color corresponds to cranial-caudal fiber direction; cranial is to the left and caudal to the right. Color image is available online at www.liebertpub.com/neu

extent of the lesion. Cranial ROI FA and MD calculations were not performed in this case. Median ROI size across the three spinal cord locations was 26 pixels and ranged from 15 to 55. The FA and MD values for cases are outlined in Table 2. The FA and MD values for cranial and caudal ROI were signi cantly different from the lesion ROI ($p_a < 0.0001$). The FA but not MD values for cranial and caudal ROI were different from each other ($p_a = 0.008$, $p_a = 0.202$). Tractography revealed absence of translesional bers in four cases and partial disruption in 18 (Fig. 2C). Two of the four dogs with apparent physical transection had IVDH while the other two had vertebral column trauma resulting in fracture/luxation.

Using overall ROI for controls (combined cranial, middle, and caudal ROI), FA was signi cantly higher in controls compared with each ROI in cases ($p_a < 0.0001$) (Fig. 3A). The MD was signi cantly lower in controls compared with cranial and lesion epicenter ROI in cases ($p_a = 0.001$, $p_a < 0.0001$, respectively) (Fig. 3B). The MD in controls was also lower than MD for caudal ROI in cases, but the difference was not signi cant ($p_a = 0.237$).

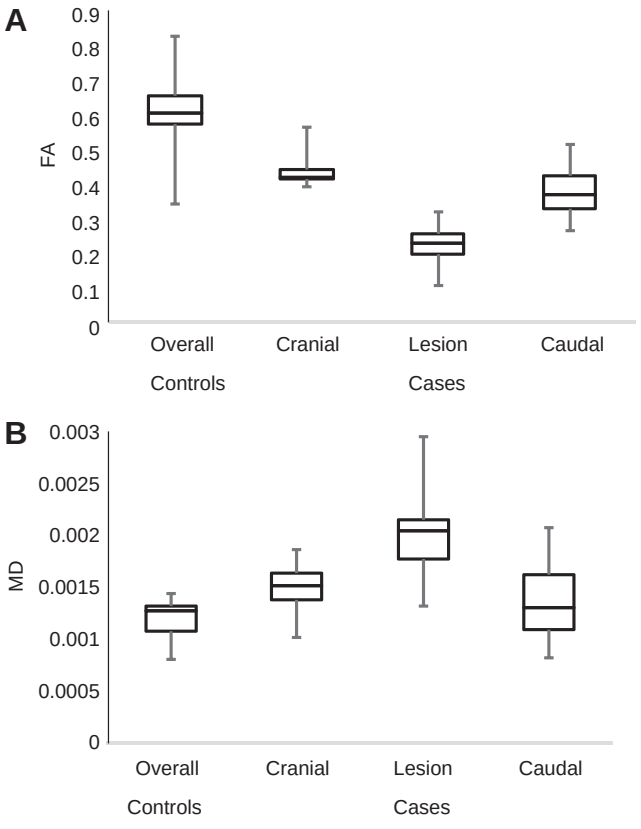

FIG. 3. The fractional anisotropy (FA) and mean diffusivity (MD) values compared between controls and cases. (A) Overall FA in controls was signi cantly different from FA for each region of interest (ROI) in cases ($p_a < 0.0001$). In cases, FA for cranial ROI and FA for caudal ROI were each signi cantly different from FA for lesion ROI ($p_a < 0.0001$). The FA for cranial ROI was signi cantly different from FA for caudal ROI ($p_a = 0.008$). (B) Overall MD in controls was signi cantly different from cranial ROI and lesion ROI in cases ($p_a = 0.001$, $p_a < 0.0001$). Overall MD in controls was not signi cantly different from MD for caudal ROI in cases ($p_a = 0.237$). In cases, MD for cranial ROI and MD for caudal ROI were each signi cantly different from MD for lesion ROI ($p_a < 0.0001$). The MD for cranial ROI was not signi cantly different from MD for caudal ROI ($p_a = 0.202$).

Age and duration of injury were variably associated with the FA and MD calculations and, thus, were included in the model when investigating associations between DTI variables and motor function. The OFS was higher for dogs with higher FA values at the lesion epicenter, but this association was no longer signi cant once corrected for multiple comparisons ($p = 0.0387$, $p_a = 0.116$) (Fig. 4A). The presence of translesional bers, as demonstrated by tractography, was associated with a higher OFS ($p = 0.0299$) (Fig. 4B).

Discussion

We established FA and MD values at the lesion epicenter in dogs with chronic SCI and demonstrated signi cant differences compared with neurologically normal dogs. Further, values calculated on areas cranial and caudal to the lesion that appeared normal on T2W images were also abnormal relative to the control population. Tractography depicted varying degrees of ber disruption at the lesion epicenter including apparent physical transection in a subset. These ndings suggest that DTI can capture microstructural degenerative changes distant from the injury site not evident on conventional MRI and identify complete structural compromise at the epicenter in dogs with severe SCI. The FA at the lesion and the presence of translesional bers were associated with hindlimb motor function. This suggests that DTI can not only establish a

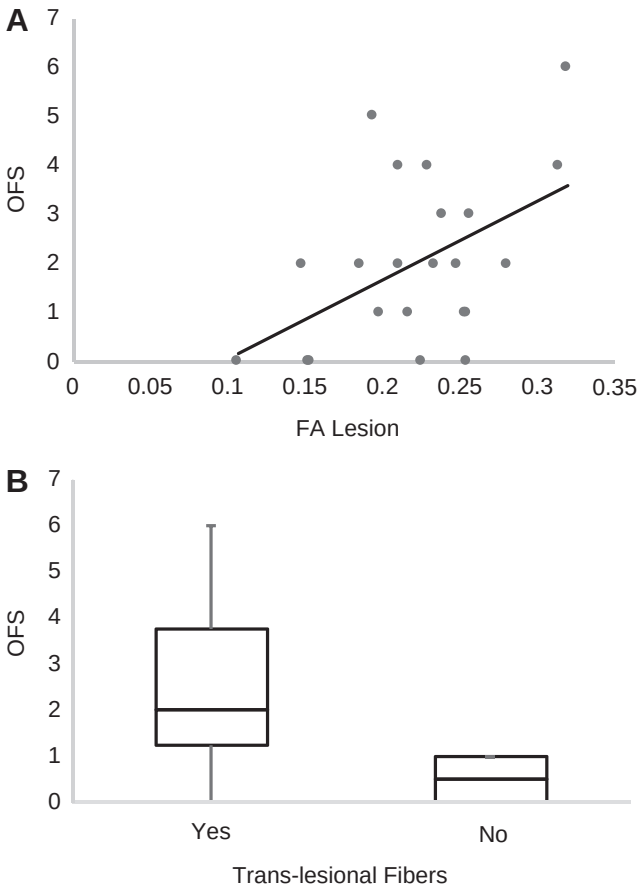

FIG. 4. Relationship between imaging ndings and gait scores. (A) Fractional anisotropy (FA) for lesion region of interest was associated with open eld score (OFS) ($p = 0.0212$, $p_a = 0.127$). (B) Presence of translesional bers was associated with OFS ($p = 0.0299$).

continuum of lesion severity and quantify lesion characteristics but also improve our understanding of motor recovery in dogs after severe thoracolumbar SCI, enhancing the utility as a model of chronic paralysis.

MRI has become standard in the assessment of the injured spinal cord and is invaluable to achieving an accurate diagnosis. Conventional MRI, however, has limited sensitivity to detect more subtle changes that occur within the spinal cord after injury. DTI provides microstructural information and has been shown to enhance detection of pathology in the spinal cord in regions that appear normal using standard sequences in persons with cervical spondylotic myelopathy and experimental rodent SCI models.[15,16,30]

Our results are consistent with this, showing abnormal DTI values relative to control dogs in normal-appearing areas of the spinal cord above and below the apparent lesion on T2W images. While our findings showed decreased FA and increased MD within and beyond the visible lesion, previous studies in dogs with SCI have found variable increases, decreases, or indistinguishable changes in these indices relative to control values.[22,24,25]

Direct comparisons are challenging, however, because the majority of dogs previously reported were evaluated at the time of an acute SCI in which the pathological changes (i.e., edema, hemorrhage, inflammation, etc.) are distinct from those that characterize the chronic injury setting (i.e., malacia, gliosis, cavitation, wallerian degeneration, demyelination). Because these were pet dogs who survived their SCI, obtaining tissue samples from the regions of spinal cord that looked normal on T2W images was not possible, and determining the precise histologic correlate for specific DTI changes is challenging.[11]

Quantitative indices, however, have been confirmed previously in experimental models to reflect a variety of histopathological changes in the chronic injury setting including malacia, gliosis, cavitation, wallerian degeneration, and demyelination.[11,33,37] This supports a similar explanation for the FA and MD changes noted in these dogs, especially the potential to capture wallerian degeneration and demyelination cranial and caudal to the visible lesion apparent on conventional MRI. The ability of DTI to reveal the degenerative changes and axonal loss that occur in areas distant from the lesion epicenter offers a sensitive way to evaluate the effects of severe injury and avoids the complex pathological changes at the lesion epicenter commonly noted on conventional MRIs that can obscure the ability to determine axonal integrity.

Tractography, which leverages the microstructural information provided by quantitative analysis to produce a visual depiction of spinal cord white matter tracts, showed varying degrees of fiber thinning and deviation from the normal cranial to caudal orientation through the area of injury in all dogs.[12,13,16,31] Four dogs had an absence of any translesional fibers, consistent with previous reports that physical spinal cord transections are rare.[38,40] Because all 22 dogs were judged to be clinically complete based on loss of pain perception and had severe lesions evident on conventional MRI, tractography might be useful to identify cases with spinal cord transection. While two of the four dogs had severe luxation, the other two had IVDH suggesting that transection can occur secondary to etiologies other than trauma.

Because transection was not confirmed histologically in any of the four dogs and there are limitations to the sensitivity of tractography, especially at lower SNR, it is possible that our findings reflected the inability to detect connections spanning the lesion rather than confirming their absence. It is also possible, given the relatively large and anisotropic voxel size, that partial volume averaging led to errors in estimating fiber direction or density among the 18 dogs with at least some translesional fibers. The four dogs with absent connections on tractography, however, all remained completely paralyzed and had among the most abnormal FA values at the lesion epicenter supporting that they had the most severe injuries among this population. The ability of DTI to identify varying degrees of fiber disruption upward of physical transection and to quantify degenerative changes improves the characterization of the spectrum of injury severity that occurs among dogs with naturally occurring, severe SCI and underscores the overlap between canine and human SCI.

The FA at the lesion epicenter and the presence of translesional connections depicted via tractography were each associated positively with OFS, although the relationship between FA and gait was no longer significant after correction for multiple comparisons. Similar reports in people have shown that FA and other DTI parameters correlated with function, suggesting that quantitative analysis, particularly FA, might provide clinically relevant information on motor function in dogs with SCI.[11,14,17,18]

While we did not establish cutoff values for FA or MD (or explore the utility of other DTI indices) that could predict motor function, DTI along with other newer MRI applications (e.g., functional MRI) may produce useful noninvasive injury biomarkers capable of relating structural severity to function.[11,14,17] Further, for dogs with no translesional fibers, taken to mean there was a spinal cord transection, the association with worse gait scores implies that at least some supraspinal influence might play a role in functional motor recovery in dogs after severe, spontaneous SCI. This is supported by reports in people and animal models on the role of residual supraspinal input on regaining locomotion after injury.[41,42]

Historically, dogs that regain ambulation but not pain perception after clinically complete SCI are labeled as "spinal walkers" exhibiting purely reflexive movement generated by intraspinal circuitry contained below the level of injury. Our findings suggest that interplay between residual supraspinal influence and the intraspinal circuitry that produces reflexive stepping might be important.[43,46] The identification of translesional connections on imaging, however, does not differentiate between functional and nonfunctional axons. It is also unclear how many intact axons are needed to interact with intraspinal motor circuitry to result in meaningful function below the level of injury.

We have shown previously that the presence of translesional motor conduction in a similar population of dogs was associated with hindlimb motor function.[47] This offers additional support that functional connections delivering supraspinal input are present in some dogs with severe lesions and likely contribute to regaining independent ambulation after injury. DTI complements other means of evaluation such as electrodiagnostic testing in dogs with incomplete recovery after severe SCI. Further investigation of the relationship between residual structure and function focused on development of DTI indices as noninvasive biomarkers of motor recovery has important applications for both canine and human SCI.

The main limitation of this study is the relatively low SNR that is, in part, because of the limitations of an older 1.5T magnet. We optimized the signal by having a relatively large number of directions (35) and increasing the slice thickness producing images of acceptable quality. We compared SCI dogs and normal dogs using the same protocol allowing direct comparison of the measured values. The FA and MD values have also been found to be relatively constant across different magnet field strengths with a trend toward overestimation of FA at a lower SNR.[48,49] Our tractography results were more strongly affected by low SNR and should be interpreted with caution. We used a simple diffusion tensor model

that is robust to low SNR, however. We also just looked at the presence or absence of translesional fibers in these dogs rather than attempting to quantify the number of spanning fibers. Other limitations include the small sample size, lack of interobserver reliability, and lack of histopathological samples to confirm imaging findings.

Overall, we demonstrated the utility of quantitative and qualitative DTI analyses to better characterize the spectrum of lesion severity, specifically the extent of spinal cord degeneration distant from the lesion and the structural continuity at the epicenter, in dogs with chronic impairment after severe SCI. These findings emphasize the lesion complexity within this population and highlight the similarities between dogs with naturally occurring SCI and humans with SCI. Our results also provide clues regarding the association between motor recovery and structural spinal cord integrity and might allow identification of subsets among severely injured individuals with differing potential for recovery or differing ability to respond to certain interventions. This has implications for clinical trial design and supports the use of the chronically paralyzed dogs to investigate potential therapies for chronically paralyzed humans.

Acknowledgments

T32 OD011130 - Comparative Medicine and Translational Research Training Program.

Author Disclosure Statement

No competing financial interests exist.

References

1. Granger, N., Carwardine, D. (2014). Acute spinal cord injury tetraplegia and paraplegia in small animals. Vet. Clin. Small Anim. Pract. 44, 1131–1156
2. Olby, N.J., Levine, J., Harris, T., Muñana, K., Skeen, T., and Sharp, N. (2003). Long-term functional outcome of dogs with severe injuries of the thoracolumbar spinal cord: 87 cases (1996–2001). J. Am. Vet. Med. Assoc. 222, 762–769.
3. Olby, NJ. (2010). The pathogenesis and treatment of acute spinal cord injuries in dogs. Vet. Clin. Small Anim. Pract. 40, 791–807.
4. Boekhoff, T.M., Flieshardt C., Ensinger, E.M., Fork, M., Kramer, S., and Tipold A. (2012). Quantitative magnetic resonance imaging characteristics: evaluation of prognostic value in the dog as a translational model for spinal cord injury. J. Spinal Disord. Tech. 25, E81–E87.
5. De Risio, L., Adams, V., Dennis, R., and McConnell, F.J. (2009). Association of clinical and magnetic resonance imaging findings with outcome in dogs with presumptive acute noncompressive nucleus pulposus extrusion: 42 cases (2000–2007). J. Am. Vet. Med. Assoc. 234, 495–504.
6. Griffin, J.F., Davis, M.C., Ji, J.X., Cohen, N.D., Young, B.D., and Levine J.M. (2015). Quantitative magnetic resonance imaging in a naturally occurring canine model of spinal cord injury. Spinal Cord 53, 278–284.
7. Ito, D., Matsunaga, S., Jeffery, ND., Sasaki, N., Nishimura, R., Mochizuki, M., Kasahara, M., Fujiwara, R., and Ogawa, H. (2005). Prognostic value of magnetic resonance imaging in dogs with paraplegia caused by thoracolumbar intervertebral disk extrusion: 77 cases (2000–2003). J. Am. Vet. Med. Assoc. 227, 1454–1460.
8. Levine, J.M., Fosgate, G.T., Chen, A.V., Rushing, R., Nghiem, P.P., Platt, S.R., Bagley, R.S., Kent, M., Hicks, D.G., Young, B.D., and Schatzberg, S.J. (2009). Magnetic resonance imaging in dogs with neurologic impairment due to acute thoracic and lumbar intervertebral disk herniation. J. Vet. Intern. Med. 23, 1220–1226.
9. Basser, P.J., Mattiello, J., and LeBihan, D. (1994). MR diffusion tensor spectroscopy and imaging. Biophys. J. 66, 259–267.
10. Ito, R., Mori, S., and Melhem, E.R. (2002). Diffusion tensor brain imaging and tractography. Neuroimaging Clin. N. Am. 12, 1–19.
11. Vedantam, A., Jirjis, M.B., Schmit, B.D., Wang, M.C., Ulmer, J.L., and Kurpad, S.N. (2014). Diffusion tensor imaging of the spinal cord: insights from animal and human studies. Neurosurgery 74, 1–8.
12. Basser, P.J., Pajevic, S., Pierpaoli, C., Duda, J., and Aldroubi, A. (2000). In vivo fiber tractography using DT-MRI data. Magn. Reson. Med. 44, 625–632.
13. Ducreux, D., Fillard, P., Facon, D., Ozanne, A., Lepeintre, J., Renoux, J., Tadie, M., and Lasjaunias, P. (2007). Diffusion tensor magnetic resonance imaging and fiber tracking in spinal cord lesions: current and future indications. Neuroimaging Clin. N. Am. 17, 137–147.
14. Kelley, B.J., Harel, N.Y., Kim, C.Y., Papademetris, X., Coman. D., Wang, X., Hasan, O., Kaufman, A., Globinsky, R., Staib, LH., Cafferty, W., Hyder, F., and Strittmatter, S.M. (2014). Diffusion tensor imaging as a predictor of locomotion function after experimental spinal cord injury and recovery. J. Neurotrauma 31, 1363–1373.
15. Demir, A., Ries, M., Vital, J.M., Dehais, J., Arne, P., Caille, J.M., and Dousset, V. (2003). Diffusion-weighted MR imaging with apparent diffusion coefficient and apparent diffusion tensor maps in cervical spondylotic myelopathy. Radiology 229, 37–43.
16. Facon, D., Ozanne, A., Fillard, P., Lepeintre, J.F., Tournoux-Facon, C., and Ducreux, D. (2005). MR diffusion tensor imaging and fiber tracking in spinal cord compression. AJNR Am. J. Neuroradiol. 26, 1587–1594.
17. Peterson, J.A., Wilm, B.J., von Meyenburg, J., Schubert, M., Seifert, B., Najaf Y., Dietz, V., and Kollias, S. (2012). Chronic cervical spinal cord injury: DTI correlates with clinical and electrophysiological measures. J. Neurotrauma 29, 1556–1566.
18. Ellingson, B.M., Ulmer, J.L., Kurpad, S.N., and Schmit, B.D. (2008). Diffusion tensor MR imaging in chronic spinal cord injury. AJNR Am. J. Neuroradiol. 29, 1976–1982.
19. Koskinen, E., Brander, A., Hakulinen, U., Luoto, T., Helminen, M., Ylinen, A., and Ohman, J. (2013). Assessing the state of chronic spinal cord injury using diffusion tensor imaging. J. Neurotrauma 30, 1587–1595.
20. Schwartz, E.D., Duda, J., Shumsky, J.S., Cooper, E.T., and Gee, J. (2005). Spinal cord diffusion tensor imaging and fiber tracking can identify white matter tract disruption and glial scar orientation following lateral funiculotomy. J. Neurotrauma 22, 1388–1398.
21. Griffin, J.F. IV, Cohen, N.D., Young, B.D., Eichelberger, B.M., Padua, A. Jr., Purdy, D., and Levine, J.M. (2013). Thoracic and lumbar spinal cord diffusion tensor imaging in dogs. J. Magn. Reson. Imaging 37, 632–641.
22. Pease, A., and Miller, R. (2011). The use of diffusion tensor imaging to evaluate the spinal cord in normal and abnormal dogs. Vet. Radiol. Ultrasound 52, 492–497.
23. Yoon, H., Park, N.W., Ha, Y.M., Kim, J., Moon, W.J., and Eom, K. (2016). Diffusion tensor imaging of white and grey matter within the spinal cord of normal Beagle dogs: sub-regional differences of the various diffusion parameters. Vet. J. 215, 110–117.
24. Konishi, Y., Satoh, H., Kuroiwa, Y., Kusaka, M., Yamashita, A., Asada, Y., and Asanuma T. (2017). Application of fiber tractography and diffusion tensor imaging to evaluate spinal cord diseases in dogs. J. Vet. Med. Sci. 79, 418–424.
25. Wang-Leandro, A., Siedenburg, J.S., Hobert, M.K., Dziallas, P., Rohn, K., Stein, V.M., and Tipold, A. (2017). Comparison of preoperative quantitative magnetic resonance imaging and clinical assessment of deep pain perception as prognostic tools for early recovery of motor function in paraplegic dogs with intervertebral disc herniations. J. Vet. Intern. Med. 31, 842–848.
26. Olby, N.J., De Risio, L., Muñana, K.R., Wosar, M.A., Skeen, T.M., Sharp, N.J., and Keene, B.W. (2001). Development of a functional scoring system in dogs with acute spinal cord injuries. Am. J. Vet. Res. 62, 1624–1628.
27. Olby, N.J., Muguet-Chanoit, A.C., Lim, J.H., Davidian, M., Mariani, C.L., Freeman, A.C., Platt, S.R., Humphrey, J., Kent, M., Giovanella, C., Longshore, R., Early, P.J., and Munana, K.M. (2016). A placebo-controlled, prospective randomized clinical trial of polyethylene glycol and methylprednisolone sodium succinate in dogs with intervertebral disk herniation. J. Vet. Intern. Med. 30, 206–214.
28. Seiler, G.S., Robertson, I.D., Mai, W., Widmer, W.R., Suran, J., Nemanic, S., Lamb, C.R., Lang, J., Johnson, J.L., and Thrall, D.E. (2012). Usefulness of a half-fourier acquisition single-shot turbo spin-echo pulse sequence in identifying arachnoid diverticula in dogs. Vet. Radiol. Ultrasound 53, 157–161.

29. Jones, D.K., Williams, S., Gasston, D., Horsfield, M.A., Simmons, A., and Howard, R. (2002). Isotropic resolution diffusion tensor imaging with whole brain acquisition in a clinically acceptable time. Hum. Brain Mapp. 15, 216–230.
30. Ford, J.C., Hackney, D.B., Alsop, D.C., Jara, H., Joseph, P.M., Hand, C.M., and Black, P. (1994). MRI characterization of diffusion coefficients in a rat spinal cord injury model. Magn. Reson. Med. 31, 488–494.
31. Ries, M., Jones, R.A., Dousset, V., and Moonen, C.T. (2000). Diffusion tensor MRI of the spinal cord. Magn. Reson. Med. 44, 884–892.
32. Sundberg, L.M., Herrera, J.J., and Narayana, P.A. (2010). In vivo longitudinal MRI and behavioral studies in experimental spinal cord injury. J. Neurotrauma 27, 1753–1767.
33. Ellingson, B.M., Schmit, B.D., and Kurpad, S.N. (2010). Lesion growth and degeneration patterns using diffusion tensor 9.4-T magnetic resonance imaging in rat spinal cord injury. J. Neurosurg. Spine 13, 181–192.
34. Budde, M.D., Kim, J.H., Liang, H.F., Schmidt, R.E., Russell, J.H., Cross, A.H., and Song, S.K. (2007). Toward accurate diagnosis of white matter pathology using diffusion tensor imaging. Magn. Reson. Med. 57, 688–695.
35. Herrera, J.J., Chacko, T., and Narayana, P.A. (2008). Histological correlations of diffusion tensor imaging metrics in experimental spinal cord injury. J. Neurosci. Res. 86, 4430–4437.
36. Kozlowski, P., Raj, D., Liu, J., Lam, C., Yung, A.C., and Tetzlaff, W. (2008). Characterizing white matter damage in rat spinal cord with quantitative MRI and histology. J. Neurotrauma 25, 653–676.
37. Zhang, J., Jones, M., DeBoy, CA., Reich, D.S., Farrell, J., Hoffman, P.N., Griffin, J.W., Sheikh, K.A., Miller, M.I., Mori, S., and Calabresi, P.A. (2009). Diffusion tensor magnetic resonance imaging of Wallerian degeneration in rat spinal cord after dorsal root axotomy. J. Neurosci. 29, 3160–3171.
38. Griffiths, I.R. (1978). Spinal cord injuries: a pathological study of naturally occurring lesions in the dog and cat. J. Comp. Pathol. 88, 303–315.
39. Kakulas, B.A., and Kaelan, C. (2015). The neuropathological foundations for the restorative neurology of spinal cord injury. Clin. Neurol. Neurosurg. 129, S1–7.
40. Smith, P.M., and Jeffery, N.D. (2006). Histological and ultrastructural analysis of white matter damage after naturally-occurring spinal cord injury. Brain Pathol. 16, 99–109.
41. Field-Fote, E.C., Yang, J.F., Basso, D.M., and Gorassini, M.A. (2017). Supraspinal control predicts locomotor function and forecasts responsiveness to training after spinal cord injury. J. Neurotrauma 34, 1813–1825.
42. Van den Brand, R., Heutschi, J., Barraud, Q., DiGiovanna, J., Bartholdi, K., Huerlimann, M., Friedli, L., Vollenweider, I., Moraud, E.M., Duis, S., Dominici, N., Micera, S., Musienko, P., and Courtine, G. (2012). Restoring voluntary control of locomotion after paralyzing spinal cord injury. Science 336, 1182–1185.
43. Blauch, B. (1977). Spinal reflex walking in the dog. Vet. Med. Small Anim. Clin. 72, 1696–1673.
44. Handa, Y., Naito, A., Watanabe, S., Komatsu, S., and Shimizu, Y. (1986). Functional recovery of locomotive behavior in the adult spinal dog. Tohoku J. Exp. Med. 148, 373–384.
45. Gallucci, A., Dragone, L., Menchetti, M., Gagliardo, T., Pietra, M., Cardinali, M., and Gandini, G. (2017). Acquisition of involuntary spinal locomotion (spinal walking) in dogs with irreversible thoracolumbar spinal cord lesions: 81 dogs. J. Vet. Intern. Med. 31, 492–497.
46. Naito, A., Shimizu, Y., and Handa, Y. (1990). Analyses of airstepping movement in adult spinal dogs. Tohoku J. Exp. Med. 162, 41–48.
47. Lewis, M.J., Howard, J.F. Jr., and Olby, N.J. (2017). The relationship between trans-lesional conduction, motor neuron pool excitability, and motor function in dogs with incomplete recovery from severe spinal cord injury. J. Neurotrauma 34, 1–9.
48. Farrell, J.A., Landman, B.A., Jones, C.K., Smith, S.A., Prince, J.L., van Zijl, P.C., and Mori, S. (2007). Effects of signal-to-noise ratio on the accuracy and reproducibility of diffusion tensor imaging-derived fractional anisotropy, mean diffusivity, and principal eigenvector measurements at 1.5 T. J. Magn. Reson. Imaging 26, 756–767.
49. Polders, D.L., Leemans, A., Hendrikse, J., Donahue, M.J., Luijten, P.R., and Hoogduin, J.M. (2011). Signal to noise ratio and uncertainty in diffusion tensor imaging at 1.5, 3.0, and 7.0 Tesla. J. Magn. Reson. Imaging 33, 1456–1463.

Address correspondence to:
Natasha J. Olby, Vet MB, PhD
Department of Clinical Sciences
College of Veterinary Medicine
North Carolina State University
1060 William Moore Drive
Raleigh, NC 27607

E-mail: njolby@ncsu.edu